ISSN 1070-3284, Russian Journal of Coordination Chemistry, 2016, Vol. 42, No. 8, pp. 502–508. © Pleiades Publishing, Ltd., 2016.

Anion-Directed Assembly of Two Novel Cadmium(II) Complexes Containing 2,2'-(1,4-Propylene)bis(1*H*-Benzimidazole) Ligand[1]

Y. Wang[a], * and L. L. An[b]

[a] *Department of Chemistry and Chemical Engineering, Baoji University of Arts and Science, Baoji, Shaanxi, 721013 P.R. China*
[b] *School of Chemical Engineering, Northwest University for Nationalities, Lanzhou, 730030 P.R. China*
**e-mail: wangyan7144279@163.com*

Received August 29, 2015

Abstract—Two novel inorganic-organic hybrids, $\{[Cd(C_3BIm)(Bdc)] \cdot H_2O\}_n$ (**I**) and $\{[Cd(C_3BIm)(Btc)] \cdot 4H_2O\}_n$ (**II**) $\{H_2C_3BIm$ = 2,2'-(1,3-propylene)bis(1*H*-benzimidazole), H_2Bdc = benzene-1,3-dicarboxylic acid, and H_3Btc = benzene-1,3,5-tricarboxylic acid$\}$, have been prepared under specific reaction temperature and ratio of reactants. Their characterization included IR, TGA, and single-crystal X-ray diffraction analysis (CIF files CCDC. nos. 801661 (**I**), 801662 (**II**)). Both complexes **I** and **II** exhibit two-dimensional puckered hexagonal (6,3) sheets structurally, whose 3-connecting nodes are provided by H_2C_3BIm, H_2Bdc, Cd^{2+} (**I**) and H_2C_3BIm, H_2Btc, Cd^{2+} (**II**), respectively. Furthermore, both compounds show intense luminescence at room temperature.

DOI: 10.1134/S1070328416080066

INTRODUCTION

Recently, growing efforts have been directed toward coordination polymers, because of their potential applications as functional materials in gas adsorption and separation, catalytic conversion, optoelectronics, luminescence, and magnetism, as well as their intriguing topologies [1–10]. Most coordination polymers are constructed using appropriate organic ligands, especially bridged ligands containing oxygen and nitrogen atoms, to coordinate with metal centers [11, 12]. In this regard, bis(2-benzimidazoles) and certain substituted bis(2-benzimidazolyl)-alkanes are attractive ligand choices because of their multifunctional linking groups. Many complexes based on these ligands have been reported, owing to their wide-ranging antivirus activity [13, 14], coordination chemistry in the context of simulating biological systems [8], and importance in selective ion exchange resins [9, 10]. In the metal-C_3BIm system, metal center structures of copper [11], nickel [12], and cobalt [13] have been widely reported. However, H_2C_3BIm complexes of cadmium with high-dimensional frameworks are relatively rare in the literature. As such, our groups have been interested in complexes bridged through H_2C_3BIm and other auxiliary ligands with a specific focus on their structures and properties. On the other hand, d^{10} metal (Zn or Cd) complexes have attracted extensive research interest in recent years for their non-linear optical, high transparency in the UV region, and fluorescence properties [14–17].

In this communication, we report the synthesis and fluorescence properties of two interesting coordination polymers: a 2D sheet $\{[Cd(C_3BIm)(m\text{-}Bdc)] \cdot H_2O\}_n$ (**I**) and a 2D sheet $\{Cd(C_3BIm)(Btc)\}_n$ (**II**). Both complexes were synthesized from a Cd salt precursor and the H_2C_3BIm ligand under hydrothermal reaction conditions. The only difference between the two reactions was the use of the auxiliary ligand, where H_2Bdc was used for complex **I**, whereas H_3Btc for complex **II**. This work demonstrates that different auxiliary ligands used in certain reactions may play a major role in the products.

EXPERIMENTAL

Materials and physical measurements. All chemicals for syntheses and analyses were commercially purchased and used without further purification. The H_2C_4BIm, H_2C_3BIm, H_2Bdc, and H_3Btc ligands were prepared according to the reported method [18]. Elemental analyses (C, H, and N) were performed on a Perkin-Elmer 2400CHN Elemental Analyzer. The emission/excitation spectra were recorded on a Varian Cary Eclipse spectrometer. TG analyses were performed on a Perkin-Elmer TGA instrument in flowing N_2 at a heating rate of 10°C min^{-1}. Powder X-ray diffraction (PXRD) analysis of the sample was carried out on a SHIMADZU XRD-6100 X-ray diffractometer with CuK_α (λ = 0.15418 nm) radiation.

---

[1] The article is published in the original.

Synthesis I. A mixture of $Cd(CH_3COO)_2 \cdot 2H_2O$ (0.080 g, 0.30 mmol), H_2C_3BIm (0.059 g, 0.30 mmol), H_2Bdc (0.053 g, 0.30 mmol), and H_2O (10 mL) was heated at 165°C for 3 days in a 25 mL Teflon-lined stainless steel vessel under autogenous pressure. After the reaction mixture was allowed to slowly cool down to room temperature, colorless prism-like crystals were produced with yield of 70%.

For $C_{25}H_{22}N_4O_5Cd$ (**I**) (M = 570.88)

anal. calcd., %:	C, 52.59;	H, 3.85;	N, 9.81.
Found, %:	C, 52.60;	H, 3.77;	N, 9.70.

IR (KBr; ν, cm^{-1}): 3635 s, 3118 m, 1950 s, 1786 s, 1608 w, 1575 m, 1480 m, 1449 w, 1359 w, 1308 m, 1280 m, 1265 m, 1244 m, 1227 m, 1093 s, 1074 m, 1048 s, 1004 s, 939 s, 907 s, 864 s, 850 s, 840 s, 831 s, 784 m, 766 m, 749 w, 658 m, 557 s, 505 s, 491 s, 436 w.

Synthesis II. Similar to complex I, a mixture of $Cd(CH_3COO)_2 \cdot 2H_2O$ (0.080 g, 0.30 mmol), H_2C_3BIm (0.059 g, 0.30 mmol), H_3BTC (0.063 g, 0.30 mmol), and H_2O (10 mL) was heated at 165°C for 3 days in a 25 mL Teflon-lined stainless steel vessel under autogenous pressure. After the reaction mixture was allowed to slowly cool down to room temperature, colorless prism-like crystals were produced with yield of 70%.

For $C_{26}H_{17}N_4O_{10}Cd$ (**II**) (M = 657.85)

anal. calcd., %:	C, 47.47;	H, 2.58;	N, 8.51.
Found, %:	C, 49.47;	H, 2.50;	N, 8.50.

IR (KBr; ν, cm^{-1}): 3414 m, 2930 m, 2643 s, 1614 w, 1488 s, 1375 w, 1278 m, 1223 s, 1156 s, 1107 s, 1040 s, 1004 s, 940 s, 907 s, 850 s, 727 m, 694 s, 523 s, 435 s.

X-ray structure determination. X-ray diffraction measurements were performed using a Bruker APXII CCD diffractometer with graphite monochromated MoK_α (λ = 0.71073 Å) radiation at room temperature. An empirical absorption correction was performed by using the SADABS computer program. The structural model was solved using SIR-97 and completed using difference Fourier maps calculated with SHELXL-97, which was also used for the final refinement. All programs were run under the WinGX system with atomic coordinates and anisotropical thermal parameters for all non-hydrogen atoms. The hydrogen atoms of aromatic rings were included in the structure factor calculation at the idealized positions by using a riding model. The crystallographic data and experimental details for the structures **I** and **II** are summarized in Table 1, the selected bond lengths and angles are listed in Table 2.

Supplementary material for structures **I** and **II** has been deposited with the Cambridge Crystallographic Data Centre (CCDC nos. 801661 (**I**), 801662 (**II**); deposit@ccdc.cam.ac.uk or http://www.ccdc.cam.ac.uk).

RESULTS AND DISCUSSION

The single-crystal X-ray structural analysis reveals that every asymmetric unit cell of complex **I** contains one Cd(II) centre, one H_2C_3BIm ligand, one H_2Bdc ligand, and one free water molecule. As shown in Fig. 1a, each Cd(II) atom is penta-coordinated with three carboxylate oxygen atoms (Cd–O(1) 2.213, Cd–O(3) 2.318, and Cd–O(4) 2.376 Å) of two H_2BDC ligands and two nitrogen atoms (Cd–N(1) 2.244 and Cd–N(3) 2.280 Å) from two H_2C_3BIm units. For a penta-coordinated metal centre, the distortion of the structure from trigonal bipyramidal (TBP) to square pyramidal (SP) can be evaluated by the Addison distortion index $\tau = |\beta - \alpha|/60°$, α and β being the two largest angles around the central atom, where value τ in perfect polyhedra are 1.0 for TBP and 0.0 for SP. The value of τ is 0.185 for Cd(1), which indicates that the coordination environment of this atom is distorted slightly from SP [19]. Of particular interest is that the 2D sheet in the 3D side view of the network (Fig. 2a) is corrugated. Such orientation plays an important role in the formation of the three-dimensional supramolecular network through π–π stacking interactions between the H_2C_3BIm ligands with face-to-face distances of ~3.41 Å.

The asymmetric unit cell of **II** consists of one Cd(II) centre, one H_2C_3BIm unit, one H_3Btc second ligand, and four free water molecules. As show in Fig. 1b, each Cd(II) centre is irregularly hexa-coordinated with five carboxylate oxygen atoms (Cd–O(2) 2.235, Cd–O(4) 2.277, Cd–O(5) 2.297, Cd–O(3) 2.447, and Cd–O(6) 2.511 Å) of three H_3Btc ligands and one nitrogen atom (Cd–N(4) 2.229 Å) from one H_2C_3BIm unit, resulting in a distorted octahedral coordination geometry. The carboxylate oxygen atoms (O(3), O(4), and O(5)) together with the benzimidazole nitrogen atom (N(4)) form the basal plane, while the axial positions are occupied by carboxylate oxygen atoms (O(2) and O(6)). Cd–O and Cd–N bond distances in both complexes are in typical oxygen- and nitrogen-metal bond ranges, respectively [20–22]. In complex **II**, 2D spiral is revealed in Fig. 2b. The π–π stacking between the H_2C_3BIm ligands has a face-to-face distance of ~3.42 Å.

Topologically, each Cd(II) atom is attached to two H_2C_3BIm and two H_2Bdc ligands in complex **I**, which is considered a 3-connected node because two H_2C_3BIm ligands can be simplified as one linker (Fig. 3a). Meanwhile, each Cd(II) atom is attached to one H_2C_3BIm and three H_3Btc ligands in complex **II**, and both the Cd atoms and H_3Btc ligand can be defined as a 3-connected node (Fig. 3b).

Table 1. Crystallographic data and structure refinement information for complex **I** and **II**

Parameter	Value	
	I	**II**
Crystal system	Monoclinic	Orthorhombic
Space group	$P2_1/n$	*Pbca*
Temperature	293	293
a, Å	9.2774(2)	16.234(5)
b, Å	13.4324(2)	16.253(5)
c, Å	18.3173(4)	23.139(5)
β, deg	101.020(2)	90.000(5)
V, Å ^{3}	2240.57(8)	6105(3)
Z	4	8
ρ_{calcd}, g/cm^3	1.692	1.44883
μ, mm^{-1}	1.02	0.77
F(000)	1152	2632
θ Range, deg	3.0–29.2	2.9–29.2
Limiting indices h, k, l	$-12 \leqslant h \leqslant 12, -13 \leqslant k \leqslant 18, -23 \leqslant l \leqslant 15$	$-20 \leqslant h \leqslant 10, -22 \leqslant k \leqslant 15, -31 \leqslant l \leqslant 28$
Reflection collected	5183	27327
Independent reflections (R_{int})	5183 (0.020)	7423 (0.025)
Reflections with $I > 2\sigma(I)$	3797	5053
Number of parameters	316	408
Goodness-of-fit	1.062	1.046
R_1, wR_2 ($I > 2\sigma(I)$)*	0.0246, 0.0475^a	0.0443, 0.1641^b
R_1,wR_2 (all data)**	0.0396, 0.0466	0.0663, 0.1536
$\Delta\rho_{min}/\Delta\rho_{max}$, e Å^{-3}	0.38/–0.44	1.34/–0.54

* $w = 1/[\sigma^2(F_o^2) + (0.0167P)^2]$, ** $w = 1/[\sigma^2(F_o^2) + (0.1093P)^2]$, where $P = (F_o^2 + 2F_c^2)/3$.

The simulated and experimental powder XRD patterns of complexes **I** and **II** show that the peak positions are in good agreement with each other, indicative of phase purity in the products, while the differences in intensity may be attributed to the preferential orientation of the powder samples.

To study the thermal stability of complexes **I** and **II**, thermogravimetric (TG) analyses were performed on the polycrystalline samples under nitrogen atmosphere with a heating rate of 10°C min^{-1} (Fig. 4). The TG curve of complex **I** suggests that the framework collapses in the temperature range of 200–575°C, corresponding to the liberation of organic components. TG analysis of **I** reveals an initial weight loss of 28.67%, which is attributed to removal of H_2BDC ligands (calcd. 28.7%). From the shape of the curve, it can be seen that H_2C_3BIm ligands in **I** are lost in two steps at about 400 and 570°C. The observed total mass loss of 78.38% corresponds to the complete loss of organic ligands (calcd. 77.05%). The remaining weight of 22.45% corresponds well to the percentage (22.5%) of Cd and O components, indicating that the final product is CdO. The TG curve of complex **II**, on the other hand, reveals that the framework collapses in the temperature range of 115–975°C, reflecting the release of organic components. TG analysis of **I** reveals an initial weight loss of 10.86%, which is attributed to removal of crystal water (calcd. 9.73%). From the shape of the curve, it can be seen that H_2C_3BIm and H_2Btc ligands in **II** are lost at about 100 and 970°C. The observed total mass loss of 73.87% corresponds to the complete loss of organic ligands (calcd.

Table 2. Selected bond distances (Å) and angles (deg) in complexes **I** and **II***

Bond	*d*, Å	Bond	*d*, Å
		I	
Cd(1)–O(1)	2.213(1)	Cd(1)–N(1)	2.244(2)
Cd(1)–N(3)^{i}	2.280(2)	Cd(1)–O(3)^{ii}	2.318(2)
Cd(1)–O(4) ^{ii}	2.376(2)		
		II	
Cd(1)–O(4)^{i}	2.277(3)	Cd(1)–N(4)	2.229(3)
Cd(1)–O(2)	2.235(3)	Cd(1)–O(6)^{ii}	2.511(3)
Cd(1)–O(3)^{i}	2.447(3)	Cd(1)–O(5)^{ii}	2.297(3)
Angle	ω, deg	Angle	ω, deg
		I	
O(1)Cd(1)O(3)^{ii}	101.44(6)	N(1)Cd(1)O(4)^{ii}	103.15(7)
O(1)Cd(1)O(4)^{ii}	161.74	N(1)Cd(1)O(3)^{ii}	105.72(6)
N(3)Cd (1)N(1)^{i}	110.94(6)	O(3)^{ii}Cd(1)O(4)^{ii}	55.42(6)
N(3)^{i}Cd(1)O(3)^{ii}	133.96(6)	O(1)Cd(1)N(1)	108.77(6)
N(3)^{i}Cd(1)O(4)^{ii}	89.24(6)		
		II	
N(4)Cd(1)O(4)^{i}	104.98(10)	N(4)Cd(1)O(5)^{ii}	100.59(12)
N(4)Cd(1)O(2)	103.50(12)	O(4)^{i}Cd(1)O(3)^{i}	55.02(9)
N(4)Cd(1)O(6)^{ii}	98.29(11)	O(4)^{i}Cd(1)O(5)^{ii}	140.45(11)
O(4)Cd(1)O(2)^{i}	117.73(12)	O(2)Cd(1)O(3)^{i}	89.85(11)
O(4)^{i}Cd(1)O(6)^{ii}	92.64(11)	O(3)^{i}Cd(1)O(6)^{ii}	81.81(11)
O(5)^{ii}Cd(1)O(3)^{i}	59.67(11)	O(2)Cd(1)O(6)^{ii}	135.55(11)
O(2)Cd(1)O(5)^{ii}	84.14(11)	O(5)^{ii}Cd(1)O(6)^{ii}	53.78(10)
N(4)Cd(1)O(3)^{i}	159.86(11)		

* Symmetry codes: ^{i} $-x + 2, -y + 2, -z$; ^{ii} $-x + 3/2, y + 1/2, -z + 1/2$ (**I**); ^{i} $x - 1/2, y, -z - 1/2$; ^{ii} $-x + 1, y + 1/2, -z - 1/2$ (**II**).

73.5%). The remaining weight of 19.57% corresponds well to the percentage (19.52%) of Cd and O components, again indicating that the final product is CdO.

Because of the excellent luminescent properties of Cd(II), the solid-state luminescent spectra of complexes **I** and **II** were studied at room temperature in the current work. Complex **I** exhibits an emission maximum at 363 nm (λ_{ex} = 421 nm), while complex **II** at 370 nm (λ_{ex} = 458 nm). In order to understand the nature of the emission, we analyzed the photoluminescent properties of H_2Bdc, H_3Btc, and H_2C_3BIm ligands and found the strongest emission peak at

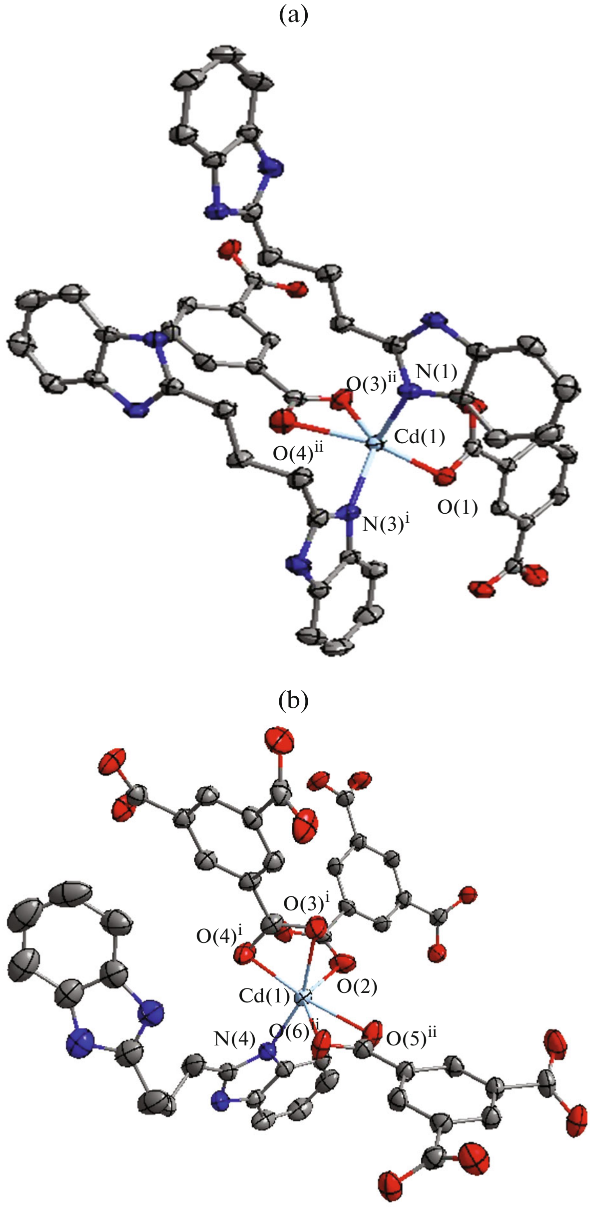

Fig. 1. Coordination environment of the Cd(II) centre in complexes **I** (a) and **II** (b) with thermal ellipsoids drawn at the 50% probability level (symmetry codes: $^{\text{i}}$ $-x + 2$, $-y + 2$, $-z$; $^{\text{ii}}$ $-x + 3/2$, $y - 1/2$, $-z + 1/2$ for **I** and $^{\text{i}}$ $x + 1/2$, y, $-z - 1/2$; $-z$; $^{\text{ii}}$ $-x + 1$, $y - 1/2$, $-z - 1/2$ for **II**). Hydrogen atoms were omitted for clarity.

280 ($\lambda_{\text{ex}} = 373$), 346 ($\lambda_{\text{ex}} = 413$) and 350 nm ($\lambda_{\text{ex}} =$ 424 nm), which may be assigned to $n \rightarrow \pi^*$ and $\pi \rightarrow \pi^*$ transitions of the intraligands. In comparison with the free ligand, the emission shift observed in complexes **I** and **II** may be attributed to ligand-to-metal charge transfer (LMCT) [23–25]. These observations demonstrate that, since they are thermally stable and insoluble in common polar and non-polar solvents, these condensed polymeric compounds have high potentials as photoactive materials.

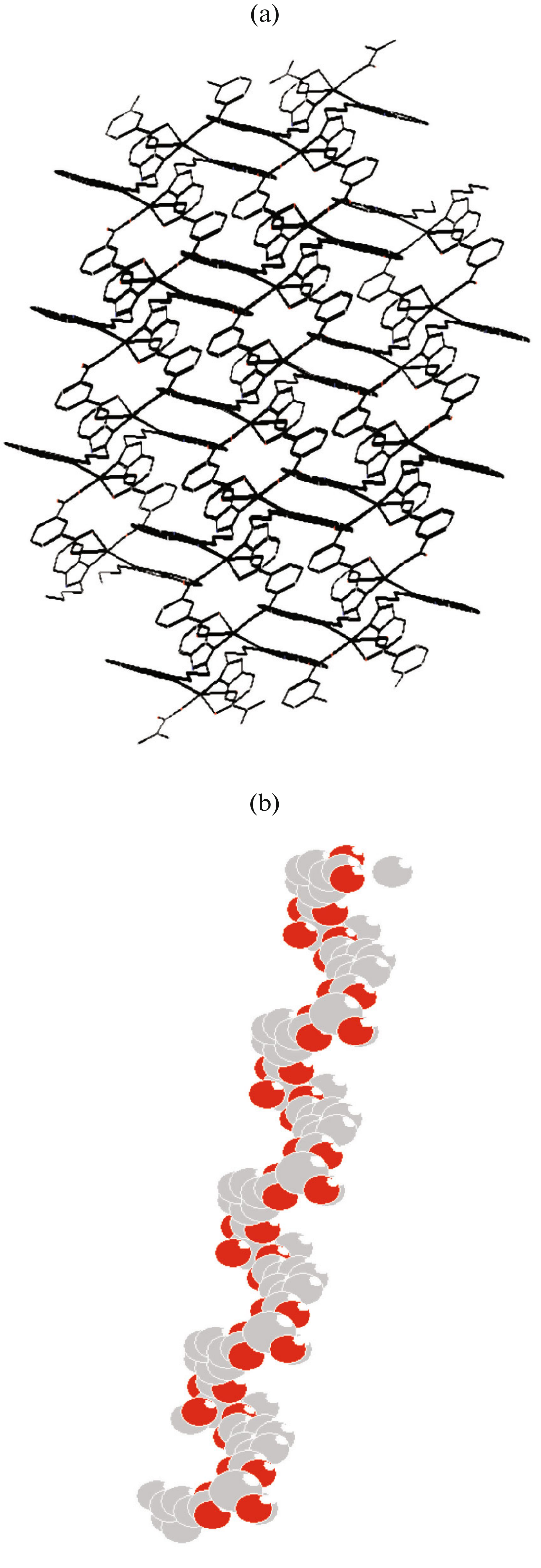

Fig. 2. 3D network of complex **I** (a) and 2D spiral of complex **II** (b).

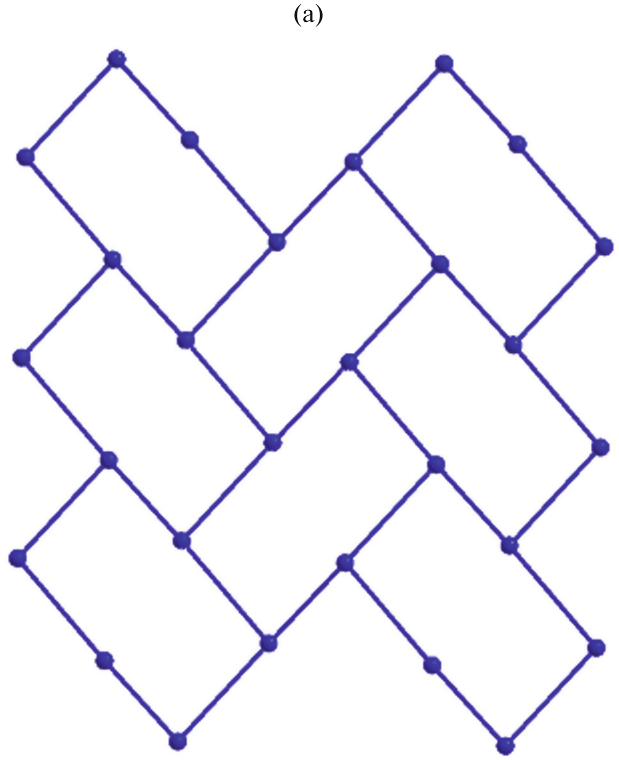

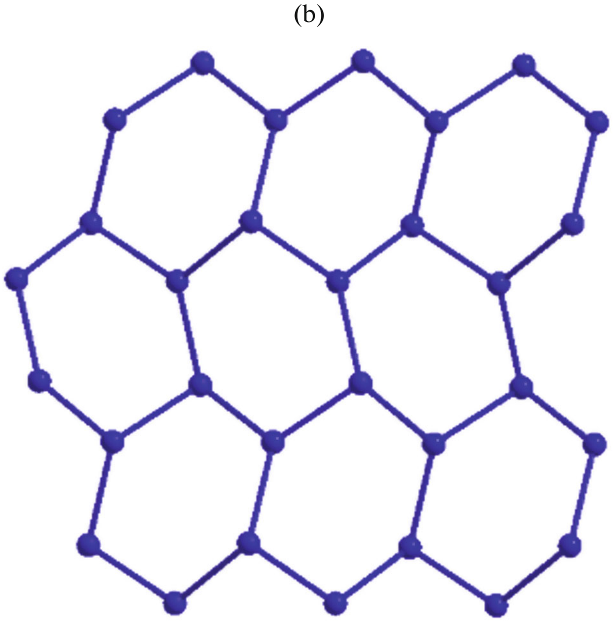

Fig. 3. Topological drawings of complexes **I** (a) and **II** (b).

ACKNOWLEDGMENTS

This work was supported by the Science and Technology Foundation of Baoji University of Arts and Science (grant no. ZK16054) and the Fundamental Research Funds for the Central Universities (grant no. 31920140103).

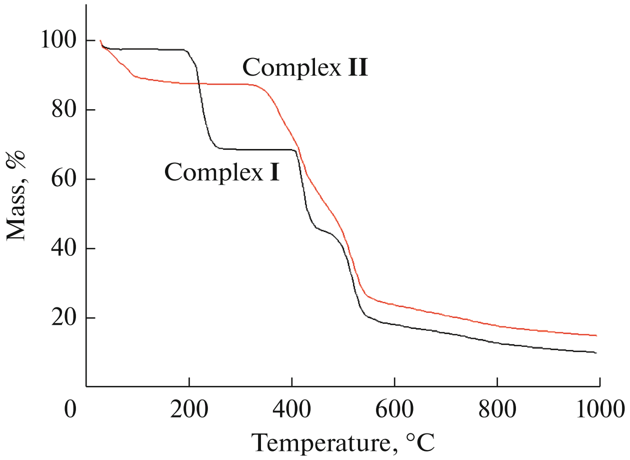

Fig. 4. TG curves of complex **I** and complex **II**.

REFERENCES

1. Rao, C.N.R., Natarajan, S., and Vaidhyanathan, R., *Angew. Chem. Int. Ed.*, 2004, vol. 43, p. 1466.
2. Ockwig, N.W., Delgado-Friederichs, O., O'Keeffe, M., et al., *Chem. Res.*, 2005, vol. 38, p. 176.
3. Tranchemontagne, D.J., Mendoza-Cortes, J.L., O'Keeffe, M., et al., *Chem. Soc. Rev.*, 2009, vol. 38, p. 1257.
4. Yoon, S. and Lippard, S.J., *J. Am. Chem. Soc.*, 2005, vol. 127, p. 8386.
5. Perry, J.J., IV, Perman, J.A., and Zaworotko, M.J., *Chem. Soc. Rev.*, 2009, vol. 38, p. 1400.
6. Wang, X.L., Qin, C., Wang, E.B., et al., *Angew. Chem., Int. Ed.*, 2007, p. 5036.
7. Wei, K.J., Ni, J., Xie, Y.S., et al., *Inorg. Chem. Commun.*, 2007, vol. 10, p. 279.
8. Fang, M., Chang, L.X., Liu, X.H., et al., *Cryst. Growth Des.*, 2009, vol. 9, p. 4006.
9. Lee, Y.G., Moon, H.R., Cheon, Y.E., et al., *Angew. Chem. Int. Ed.*, 2008, vol. 47, p. 7741.
10. Zou, H.H., Yin, X.H., Sun, X.J., et al., *Inorg. Chem. Commun.*, 2010, vol. 13, p. 42.
11. Riggio, I., Van Albada, G.A., Elis, D.D., et al., *Polyhedron*, 2001, vol. 20, p. 2659.
12. Van Albada, G.A., Kolnaar, J.J.A., Smeets, W.J.J., et al., *Eur. J. Inorg. Chem.*, 1998, p. 1337.
13. Wang, X.W., Chen, J.Z., and Liu, J.H., *Cryst. Growth Des.*, 2007, vol. 7, p. 1227.
14. Zhang, L.Y., Zhang, J.P., Lin, Y.Y., et al., *Cryst. Growth Des.*, 2006, vol. 6, p. 1684.
15. He, J.H., Yu, J.H., Zhang, Y.T., et al., *Inorg. Chem.*, 2005, vol. 44, p. 9279.
16. Tao, J., Tong, M.L., Shi, J.X., et al., *Chem. Commun.*, 2000, p. 2043.

17. Yang, E.C., Zhao, H.K., Ding, B., et al., *Cryst. Growth Des.*, 2007, vol. 7, p. 2009.
18. Zhang, S.X., Wang, H.Y., Xu, X.Y., and Lv, C.X., *Paint Coat Industry*, 2005, vol. 35, p. 4.
19. Addison, A.W., Rao, T.N., Reedijk, J., et al., *J. Chem. Soc., Dalton Trans.*, 1984, p. 1349.
20. Zou, R.Q., Bu, X.H., and Zhang, R.H., *Inorg. Chem.*, 2004, vol. 43, p. 5382.
21. Luan, X.J., Cai, X.H., Wang, Y.Y., et al., *Chem. Eur. J.*, 2006, vol. 12, p. 6281.
22. Lan, Y.Q., Li, S.L., Fu, Y.M., et al., *Dalton Trans.*, 2008, p. 6796.
23. Qin, Y.Y., Zhang, J., Li, Z.J.L., et al., *Chem. Commun.*, 2008, p. 2532.
24. Fang, Q.R., Zhu, G.S., Xue, M., et al., *Inorg. Chem.*, 2006, vol. 45, p. 3582.
25. Li, S.L., Lan, Y.Q., Ma, J.F., et al., *Cryst. Growth Des.*, 2008, vol. 8, p. 1610.